Research Paper

Toxicity Assessments of Near-infrared Upconversion Luminescent LaF₃:Yb,Er in Early Development of Zebrafish Embryos

Kan Wang[1], Jiebing Ma[1], Meng He[1], Guo Gao[1], Hao Xu[1], Jie Sang[2], Yuxia Wang[2], Baoquan Zhao[2] and Daxiang Cui[1✉]

1. Key Laboratory for Thin Film and Microfabrication of Ministry of Education, Institute of Micro-Nano Science and Technology, Shanghai Jiao Tong University, 800 Dongchuan Road, Shanghai 200240, PR China;
2. Institute of Pharmacology and Toxicology, Academy of Military Medical Sciences, 47 Taping Road , Peking 100850, PR China.

✉ Corresponding author: dxcui@sjtu.edu.cn or baoquan9838@sina.com.

Abstract

This study reports the effects of upconversion nanoparticles (UCNPs) LaF₃:Yb,Er on zebrafish, with the aim of investigating UCNPs toxicity. LaF₃:Yb,Er were prepared by an oleic acid/ionic liquid two-phase system, and characterized by transmission electron microscope and X-ray powder diffraction. 140 zebrafish embryos were divided into six test groups and one control group, and respectively were injected into 5, 25, 50, 100, 200, 400 μg/mL LaF₃:Yb,Er@SiO₂ solution, and respectively were raised for 5 days. Each experiment was repeated ten times. Results showed that water-soluble LaF₃:Yb,Er were successfully prepared, and did not exhibit obvious toxicity to zebrafish embryos under 100 μg/mL, but exhibited chronic toxicities 200 μg/mL *in vivo*, resulting in malformations and delayed hatching rate and embryonic and larval development. The excretion channels of LaF₃:Yb,Er in adult zebrafish were mainly found in the intestine after being injected evenly for 24 h. In conclusion, the exploration of LaF₃:Yb,Er for *in vivo* applications in animals and humans must consider UCNPs biocompatibility.

Key words: Upconversion nanoparticles (UCNPs), biocompatibility, toxicity, zebrafish embryo.

Introduction

In recent years, nanotechnology has emerged as a forerunner for new advances in medical research, especially in the development of drug delivery systems and *in vivo* imaging. Upconversion (UC) was recognized in the mid-1960s and has since attracted significant research interest for applications in optical devices, such as infrared quantum counter detectors and compact solid-state lasers[1, 2] Over the past decade, UC has become more prominent in biological sciences because the preparation of high-quality lanthanide-doped nanoparticles has become routine. Upconversion nanoparticles (UCNPs) can be easily coupled to proteins or other biological macromolecular systems and are used in various assays ranging from bio-detection[3-7] to cancer therapy because of their small physical dimensions and biocompatibility[8, 9]. However, lack of toxicological data on UCNPs provides difficulty in determining the risk associated with nanomaterial exposure. Thus, rapid, relevant, and efficient testing strategies must be developed to assess emerging nanomaterial concerns.

Numerous biological models have been used for toxicological assessments[10] Zebrafish were selected for this experiment because of their widespread use in

ecotoxicology[11-16], including nanoparticle toxicity assessment[17-23] The zebrafish is an aquatic vertebrate species with human homologous genes. It can be cultivated at 28 C under laboratory conditions and provide a large number of non-adherent and transparent eggs. Zebrafish are logistically attractive for rapidly evaluating integrated system effects because of their small size, rapid development, and short life cycle.

The toxicity of UCNPs has not yet been studied in zebrafish. Therefore, this study aims to study the effects of LaF$_3$:Yb,Er UCNPs solution exposure on zebrafish embryonic development at morphological and molecular levels. The potential toxicological risks of LaF$_3$:Yb,Er@SiO$_2$ were evaluated through the analysis of embryonic development, hatching, survival, and body length at several important time points as the development index.

Material and methods

Preparation and characterization of UCNPs

The synthetic principle and protocol of LaF$_3$:Yb,Er UCNPs with different components (various combinations of host materials, sensitizers, and activators) and solubilities (water-solubility and nonpolar solvents-solubility) were reported in our previous works.[26, 27] and other groups achievements[28, 29] Transmission electron microscope (TEM) and X-ray powder diffraction (XRD) were performed to investigate the morphology and structure of UNCPs. The crystalline phase of the UCNPs was studied by XRD analysis. The functional groups on the surfaces of the bare and amino-modified UCNPs (UCNPs@SiO$_2$-NH$_2$) were identified by FTIR spectroscopy and Zeta-potential test.

Zebrafish embryo toxicity study

Experimental animals

All animal experiments were performed in compliance with the local ethics committee. Zebrafish (*Danio rerio*, AB-type), approximately 7 months to 8 months old and bred in our laboratory, were used in the experiment. A 60 L glass water tank contained the aquatic environment, which was filtered by carbon. Water temperature was maintained at 28 °C ± 1 °C with a light/dark cycle of 14 h/10 h. Adult fish were fed brine shrimp three times a day. Male and female zebrafish were set up in pairs the night before injections in breeding tanks with a divider. A grid insert in the tanks allowed the eggs to fall to the bottom. The onset of light was a stimulus for the fish to mate. The dropped embryos were collected, pooled, and rinsed carefully with Holt's buffered medium several times after mating. Dead embryos were removed to avoid

test solution contamination. The embryos were observed with a microscope (Olympus, DP2-BSW, Japan) to determine the morphological effects.

Experimental design

The micropipette (O.D., 1.02 mm; I.D., 0.58 mm) with ~3 µL of LaF$_3$:Yb,Er@SiO$_2$ solution, and then mounted onto the micromanipulator holder. The eggs were arrayed in the trenches of the microinjection chamber and were oriented so that the yolk sac faced a trench wall opposite the incoming microinjection pipette (Fig. 1). The microinjection chamber was warmed to room temperature before injection. Embryos were randomly divided into groups The control group was microinjected with phenol red, whereas the other groups were microinjected with six LaF$_3$:Yb,Er@SiO$_2$ concentrations (5, 25, 50, 100, 200, 400 µg/mL). Embryos were individually injected 10 nL solution through the chorion and transferred into 6-well plates by group until 120 h post fertilized (hpf) hatched. The inclusion of phenol red aided in the detection of the injection site. The injected eggs were rinsed in a Petri dish with zebrafish embryo medium, and then incubated at 28 °C. Embryotic death, deformity, incubation period, development to 120 hpf mortality, and hatching rate were observed and recorded. The number of voluntary movement of the tail swing for each concentration (*n* = 5) in 1 min was recorded when the embryos grew to 24 hpf. The 10 s heart rate for each concentration (*n* = 5) under the microscope at 48 hpf was also recorded. The larval lengths per concentration (*n* = 5) was measured after hatching 120 hpf under the microscope. Each experiment was repeated ten times.

Biological effects of UCNPs

Zebrafish were homogenized in 1 mL phosphate buffer (0.1 M, pH 7.3). The homogenate was centrifuged at 12000 × rpm for 5 min at 4 °C. The sepn1 gene expression in AB-type zebrafish was assessed by RT-PCR performed on total RNA samples isolated from 72 hpf fish (*n* = 20), using a modified method by Deniziak *et al.*[30, 31]. Total RNA was obtained using the RNA simple Total RNA Extraction Kit (TIANGEN Biotech BEIJING CO., LTD.) according to the instructions of the manufacturer. Reverse transcription was performed using First-Strand cDNA Synthesis (Promega USA Inc). The reaction was conducted at 42 °C for 45 min, 95 °C for 5 min, and 0 °C to -5 °C for 5 min, in a 20 µL reaction mixture, containing 4 µL of 25 mM MgCl$_2$, 2 µL Reverse Transcription 10x Buffer, 2 µL 10 mM dNTP Mixture, 0.5 µL Recombinant RNasin® Ribonuclease Inhibitor, 1 µL AMV Reverse Transcriptase (High Conc.), 2 µL RNA, 1 µL random

primer, and 7.5 µL nuclease-free water to a final volume of 20 µL (Promega). Reverse transcribed cDNA (5 µL) were then amplified in a 50 µL PCR reaction, with 12.5 µL 2 x Taq PCR Master Mix, 6.5 µL nuclease-free water, 0.5 µL Upstream Control Primer, 0.5 µL Downstream Control Primer, and 25 µL paraffin oil (Promega). PCR was conducted under the following conditions: one cycle of denaturation at 94 °C for 5min, 30 cycles at 94 °C for 45 s, 65 °C for 1min, and 72 °C for 2 min; amplification was terminated by one cycle of elongation at 72 °C for 10 min. The following oligonucleotides were used in the PCR reaction: sepn-ex1, hybridizing to the three region of exon 1 (5'-GGGACTCCATCCAGCAGACG-3') and sepn-ex3, a reverse primer complementary to exon 3 (5'-TGCAGGGTCAGCGTCTCTCC-3'). Amplification products were analyzed by electrophoresis on a 1.5% agarose gel. The band intensities of the amplification products were obtained using gel documentation and analysis systems (Bio-Rad iCyclerTM System, USA).

Biodistribution in Zebrafish

Healthy adult fish were selected and anesthetized with tricaine solution (1 M/3000 V). The micropipette (O.D., 1.02 mm; I.D., 0.58 mm) was backfilled with ~4 µL of LaF_3:Yb,Er@SiO_2 solution (1 mg/mL) and was used to pierce into the pectoral fin vertically. Approximately, 2 µL solution was then injected into the heart. Zebrafish were continuously fed into the fish water at 28 °C ± 1°C for 12 h. The organs was removed and fixed with Bouin's solution, stained with Alcian Blue and made into an ultra-thin specimen, and then observed with TEM.

Statistical Analysis

Statistical tests were carried out using GraphPad Prism5 (GraphPad Software, San Diego,USA). Data hatching time, hatching success, mortality, and growth (length of larvae) were checked for normality and homogeneity of variances and complied with the requirements of parametric methods. One-way analysis of variance was used to compare the effects of the LaF_3:Yb,Er against the controls. Statistical significance was assumed with $P < 0.05$.

Results and Discussion

Characterization of UCNPs

The characterization of the obtained UCNPs in ionic liquid (IL) phase displayed good aqueous dispersion, with sizes ranging from ~7 nm to ~10 nm (Fig. 2A). However, the UCNPs aggregated after alternative centrifugation with deionized water and ethanol, indicating that the coated IL-layers were removed from the particle surfaces (Fig. 2B). The TEM image of the UCNPs in the oleic acid (OA) phase exhibited high uniformity, monodispersity, as shown in Fig. 2C. Fig. 2D and 2E showed the TEM and HR-TEM images of silica-coated UCNPs. They indicate that every UCNP was coated by a silica layer with the thickness of ~3 nm (Fig. 2E). The thickness of the silica layer could be tuned in the range of 2−20 nm by the changes of the added amount of TEOS.
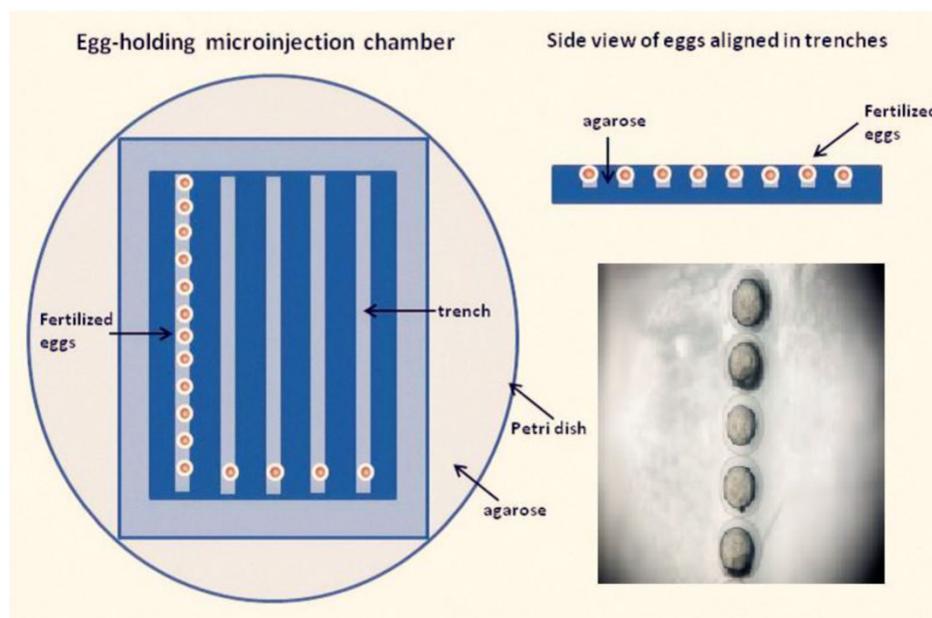
Fig 1. Zebrafish egg microinjection chamber. Fertilized zebrafish eggs are placed in the trenches of an agarose microinjection chamber and aligned in the same orientation.
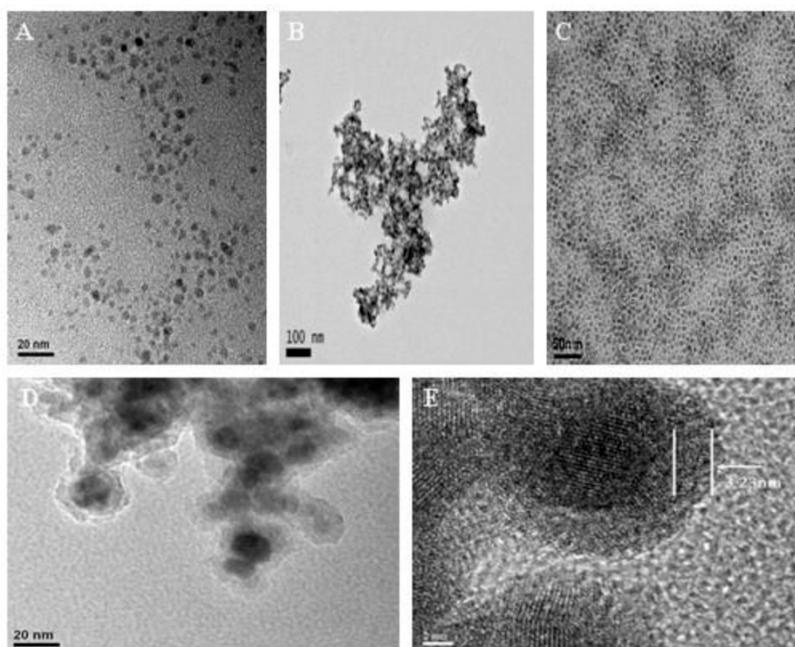
Fig 2. Transmission electron microscopy (TEM) images of the LaF$_3$:Yb,Er samples: (A,B) in ionic liquid phase (C) in oleic acid phase (D,E) TEM images of UCNPs@SiO$_2$.
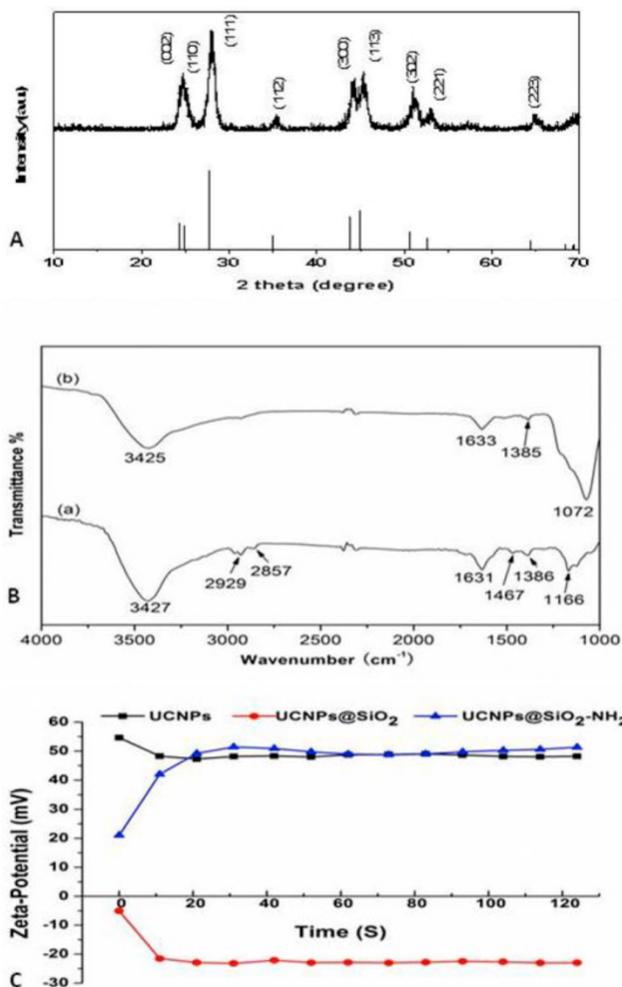
Fig 3. Characterization of upconversion nanoparticles (UCNPs). (A) X-ray diffraction (XRD) pattern of UCNPs in IL-phase. (B) Fourier transform infrared (FTIR) spectra of (a) UCNPs in IL-phase and (b) UCNPs@SiO$_2$-NH$_2$. (C) Zeta-potential of UCNPs, UCNPs@SiO$_2$, and UCNPs@SiO$_2$-NH$_2$.

The crystalline phase of the UCNPs was studied by XRD analysis (Fig. 3A). All positions and peaks of the diffraction peaks were in good agreement with the JCPDS data (No.72-1435), suggesting that the particles could be indexed to a pure hexagonal LaF$_3$ phase.

The functional groups on the surfaces of the bare and amino-modified UCNPs (UCNPs@SiO$_2$-NH$_2$) were identified by FTIR spectrometry. The bare UCNPs (Fig. 3B(a)) showed a broad band at around 3427 cm^{-1} corresponding to the O-H stretching vibration. The two peaks at 2929 cm^{-1} and 2857 cm^{-1} were the asymmetric and symmetric stretching vibrations of the methylene group in the long alkyl chain. In addition, the peaks at 1631, 1467, and 1386 cm^{-1} can be observed in the spectrum, corresponding to C-N and C-C stretching vibration of the imidazole ring. Meanwhile, a dominating peak for UCNPs@SiO$_2$-NH$_2$ (Fig. 3B(b)) appeared at 1072 cm^{-1}, indicating the existence of silica layers on the UCNPs surfaces. However, the stretching and bending vibration bands of the amine group were covered by the O-H stretching vibration band. The zeta-potential values of the three

samples: UCNPs (black line), UCNPs@SiO$_2$ (red line), and UCNPs@SiO$_2$-NH$_2$ (blue line) (Fig. 3C) in the aqueous medium were tested to further confirm the presence of amine group. The zeta-potential values of UCNPs@SiO$_2$ were all negative, with an average value of -21.34 mV because of the silica layer coating on the UCNPs surfaces. The zeta-potential values of UCNPs@SiO$_2$-NH$_2$ were all positive, with an average value of 47.15 mV. Therefore, the amine groups coupled with UCNPs successfully.

Effects of LaF$_3$:Yb,Er on development stages of zebrafish

Effects on zebrafish voluntary movement and heart rate

The earliest toxicology indicators of LaF$_3$:Yb,Er on the embryo can be observed at the 24 hpf in the zebrafish embryonic development. The number of voluntary movements of the tail swing for each concentration in 1 min was recorded. The mean of the voluntary movements for the control group was 4.5 min^{-1}. The increasing concentrations had little effect on the movements of the experimental group. The frequencies of voluntary movements in the embryo were 4.1, 3.96, 4.2, 4.6, 4.9, and 5.02 min^{-1}, respectively, as shown in Fig. 4A. The embryos showed regular heartbeats, which can be observed directly under the microscope after 48 hpf. The statistic embryonic heart rate was counted for 10 s. Fig. 4B shows, that different LaF$_3$:Yb,Er concentrations had no significant effect on the larval heart rate.

Effects on survival and hatching rate of zebrafish

Embryos for the control and experimental groups began to hatch between 48 hpf and 78 hpf. A slight effect on early hatching was visible in Fig. 5A. Hatching time and hatching success rate decreased with increasing concentrations of 5µg/mL to 400µg/mL. The survival rates of the embryos with UCNPs are shown in Fig. 5B. No significant adverse effects at lower concentrations of LaF$_3$:Yb,Er were observed on embryonic survival and development, except for the 200 µg/mL and 400 µg/mL groups.
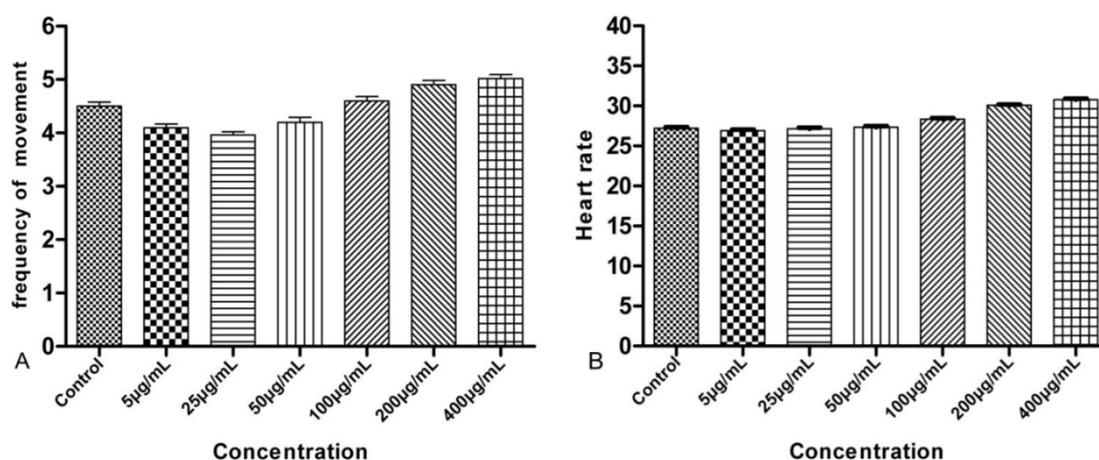
Fig 4. Frequency of voluntary movement and heart rate of the larvae. *n* = 50, 5 larvae in 10 replicates each.
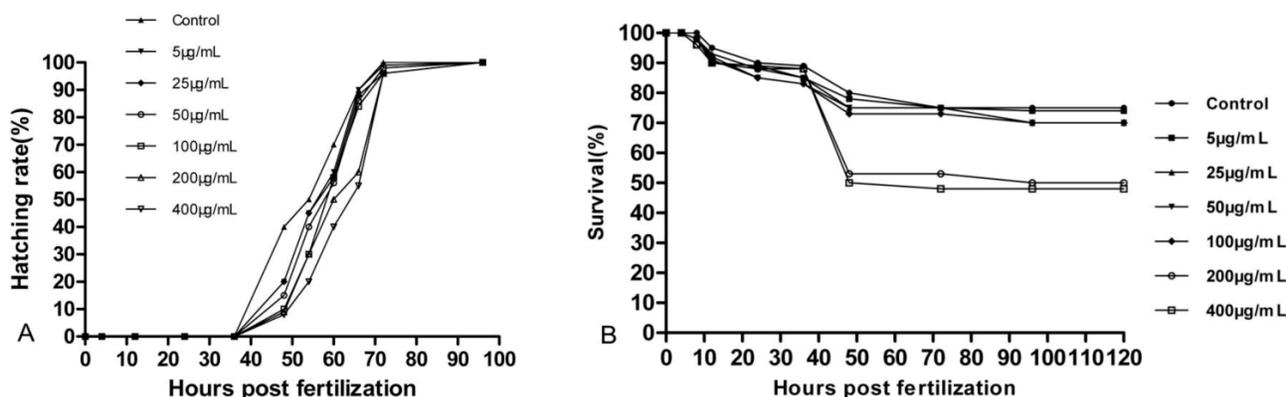
Fig 5. Survival and hatching rate of embryos. *n* = 200, 20 embryos in 10 replicates each.

Effects on larval morphology

Larval morphologies were visually inspected. Black colored eyes, vacuolated differentiating cells in the notochord, and a yolk sack equal to the volume of the head were observed in the control group. However, the injection of LaF$_3$:Yb,Er slightly shortened the larval body length and induced malformations, except in the notochords, as shown in Fig. 6 and 7. The embryos were rarely abnormal during the cleavage and gastrula period. In the control group (Fig.7 A1-2), black colored eyes, vacuolated differentiating cells in the notochord, and a yolk sack approximately equal to the volume of the head were observed. However, the experimental groups had abnormal properties in all treatment doses. The eyes were not developed in some flies and the size of the yolk sack was approximately equal to the head (Fig. 7 B1-B3). Furthermore, almost all the individuals in the UCNPs (200-400 µg/mL) exposed groups had severe morphological anomalies with embryonic development (Fig.7 C1-C5). Developmental abnormalities include non-depleted or malformed yolk; spinal, tail and caudal fin malformations; pericardial sac or yolk formations; delayed hatching; stunted body or eye growth; and edema of the body cavity, pericardial sac, or yolk sac regions. Especially, there were increased edema and weak heartbeats in the 200-400 µg/mL exposed groups than in the other doses groups.
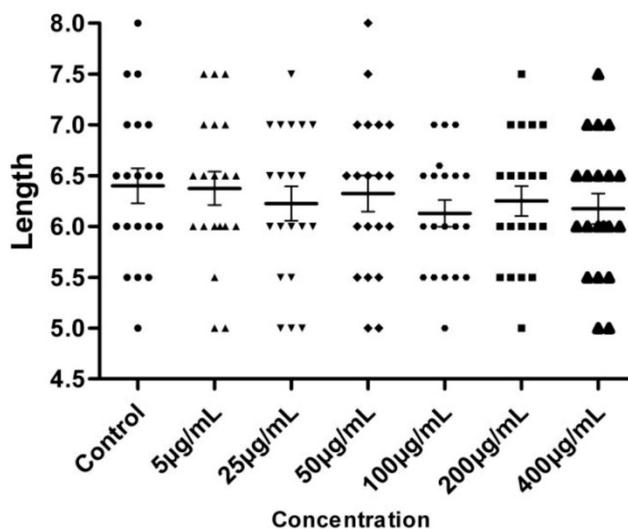
Fig 6. Larvae length after hatching. *n* = 50, 5 larvae in 10 replicates each.
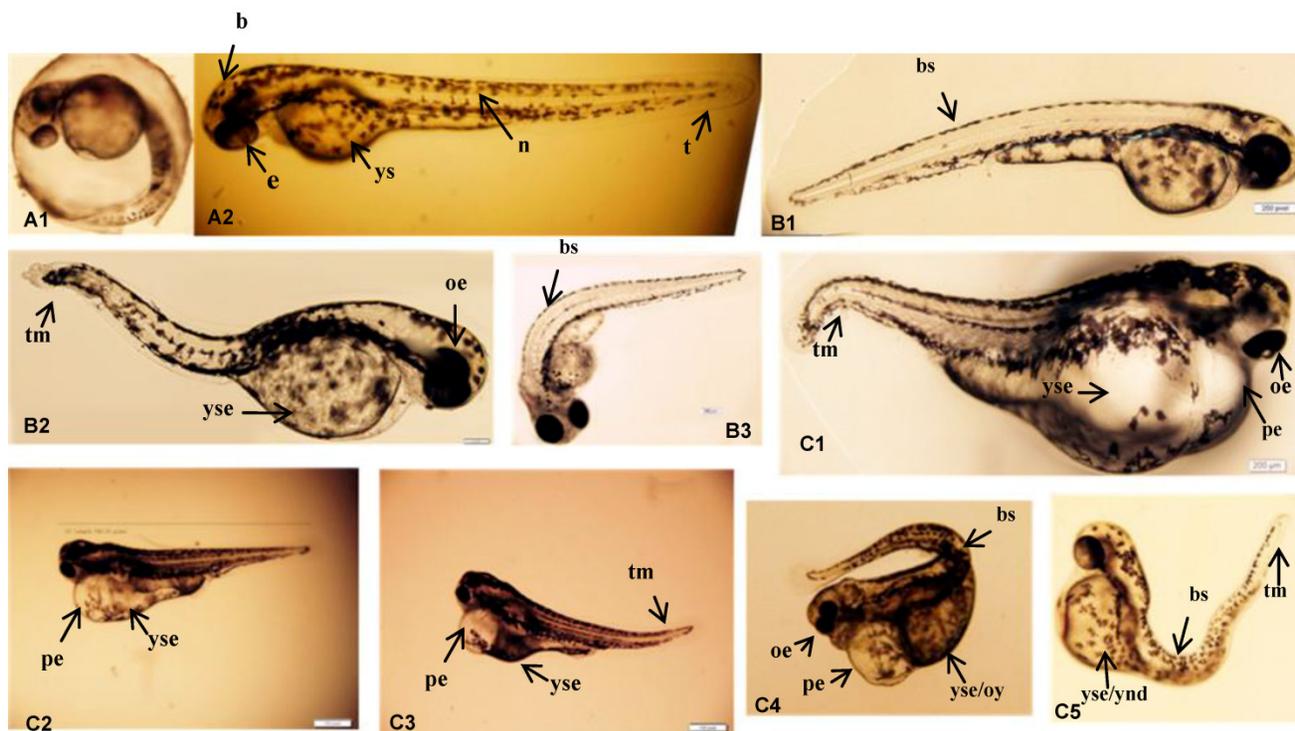
Fig 7. Phenotypic changes of zebrafish embryos at 48 hpf. (A-1, A-2) Control group. (B1-3) UCNPs<200µg/mL groups. (C1-5) UCNPs 200-400µg/mL groups. Abbreviations: b, brain; e, eye; n, notochord; t, tail; ys, yolk sac; bs, bent spine; tm, tail malformation; oe, ocular edema; pe, pericardial edema; oy, opaque yolk; yes, yolk sac edema; and ynd, yolk not depleted.
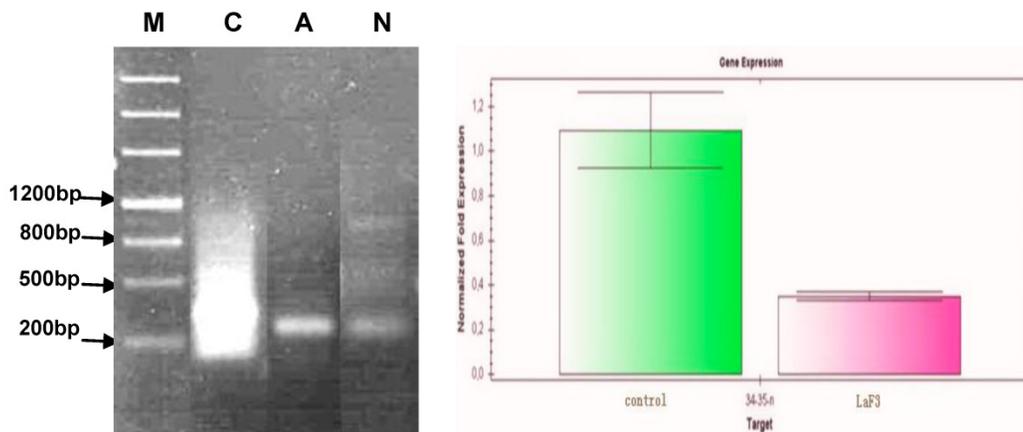
Fig 8. RT-PCR results for the sepn1 gene expression in hatched zebrafish. (A) Abbreviations: M, Marker; C, Control; A, Abnormal; N, Normal. (B) Band intensities of the amplicication products were obtained using gel documentation and analysis systems.

RT-PCR results

The sepn1 gene expression is related to abnormal notochord development and heart disease during the early developmental stages of zebrafish and humans[30] The RT-PCR results of the sepn1 gene expression in the hatched zebrafish are noted in Fig. 8A, wherein line M denotes the expression marker. The data for the control group is shown in line C. The data lanes for the exposed group that represented malformation were noted at line A. Data for zebrafish treated with LaF_3:Yb,Er solution, which did not show malformation, is shown in line N. The band intensity of the amplification products was obtained using gel documentation and analysis systems (Fig. 8B). Gene expressions were made relative to the control group by relative band intensity calculations. Values are represented as sepn1 expression ratios (n = 20). The sepn1 gene expression in the exposure groups decreased compared with that of the control group. The sepn1 expression in the exposure group was about 32% of that in the control group.

Biodistribution in Zebrafish

Ultrathin sections were prepared from the harvested zebrafish intestine for TEM imaging to observe the high accumulation levels and assess the biological effects of LaF_3:Yb,Er in zebrafish organs. The TEM images of the ultrastructural features of the intestine tissues exposed to UCNPs are shown in Fig. 9.

The LaF_3:Yb,Er mainly found in the intestine after even injection for 24 h was observed to study the excretion channels of LaF3:Yb,Er in zebrafish. Digestive enzymes can degrade intestinal *E. coli* in a short time, indicating that LaF_3:Yb,Er are bio-stable and resistant to digestive enzymes. The LaF_3:Yb,Er were well-dispersed on the intestine, but cannot be found in the cells. LaF_3:Yb,Er cannot penetrate the intestinal cell membranes by active transport or be obtained by cells through phagocytosis. Thus, the LaF_3:Yb,Er in the gut could be excreted gradually after the zebrafish with LaF_3:Yb,Er were fed during 24 h.
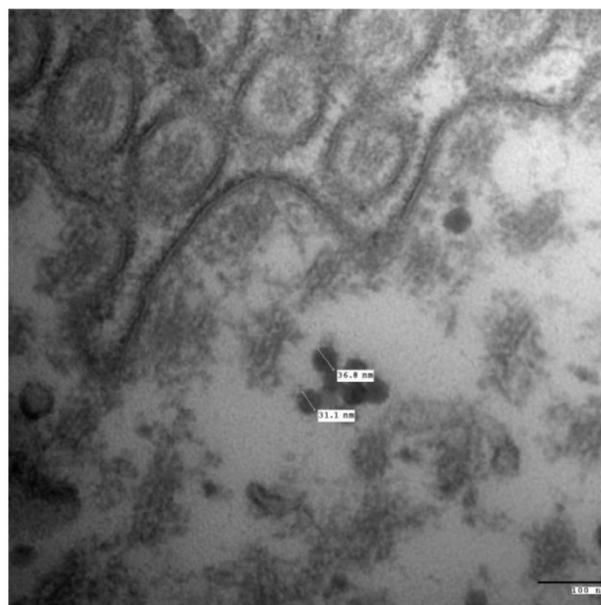
Fig 9. Transmission electron microscopy (TEM) images of the ultrastructural features of intestine tissues.

The possible mechanism of effects LaF₃:Yb,Er on zebrafish

The zebrafish model serves as a rapid and cost-effective method to conservatively assess the toxicity of novel nanopharmaceuticals. The embryos can then be exposed to the material via continuous water borne exposure or direct injection. Toxicity as-

sessment allows several parameters to be varied including concentration, nanomaterial size, chemical composition, density, exposure route, exposure time, and the point of embryonic development at which the nanomaterial is administered.

In this study, microinjection of LaF$_3$:Yb,Er UCNPs through the chorion into the yolk sac caused zebrafish embryos to develop abnormally, which may be due to La$^+$ ions binding with DNA, resulting in possible DNA damage. Bent notochords and pericardial edema were observed. The sepn1 gene expression decreased in the LaF$_3$:Yb,Er microinjection groups compared with that in the control group. Therefore, the La$^+$ ions enter the nucleus and affect gene expression, possibly causing the decreased hatching rate in the LaF$_3$:Yb,Er exposure groups in this study.

Since the toxicity of nanoparticles greatly depends on the surface modification, there was another possibility that some abnormal development of zebrafish embryos may result from the toxicity of aggregated UCNPs. It was found from the TEM images that the particle aggregate in water, so another well-recognized surface modification, such as PEG- or lipid- modified UCNPs were needed assessing.

Conclusion

Our primary studies indicated that different UCNPs LaF$_3$:Yb,Er@SiO$_2$ concentration solutions had no significant effect on larval heart rate and voluntary movement frequency. LaF$_3$:Yb,Er can produce malformations > 200 μg/mL concentrations, as well as delay hatching rate and embryonic and larval development. The excretion channels of LaF$_3$:Yb,Er in adult zebrafish were observed, and LaF$_3$:Yb,Er was mainly found in the intestine after being evenly fed for 24 h. LaF$_3$:Yb,Er exhibited low toxicity compared with other nanoparticles, which were toxic in the zebrafish model[17, 31], LaF$_3$:Yb,Er showed great potential in biological applications. UCNPs have been investigated for biomedical applications, such as cell imaging and small animal imaging[6]. Further research will focus on investigating the biocompatibility and tumor target ability of UCNPs which combined with antibody and well surface modification.

Supplementary Material

Fig.S1. http://www.thno.org/v03p0258s1.pdf

Abbreviations

TEM, transmission electron microscope; XRD, powder X-ray diffraction; UCNPs, upconversion nanoparticles.

Competing Interests

The authors report no competing interest in this work.

References

1. Wang L, Li Y. Green upconversion nanocrystals for DNA detection. Chemical Communications 2006;: 2557-2559.
2. Li C, Lin J. Rare earth fluoride nano-/microcrystals: synthesis, surface modification and application. J. Mater. Chem. 2010; 20:6831-6847.
3. Wang M, Mi CC, Wang WX, Liu CH, Wu YF, Xu ZR, Mao CB, Xu SK. Immunolabeling and NIR-excited fluorescent imaging of HeLa cells by using NaYF4: Yb, Er upconversion nanoparticles. Acs Nano. 2009; 3: 1580-1586.
4. Hu H, Xiong L, Zhou J, Li F, Cao T, Huang C. Multimodal-Luminescence Core‐Shell Nanocomposites for Targeted Imaging of Tumor Cells. Chemistry-A European Journal. 2009; 15: 3577-3584.
5. Liu Q, Sun Y, Yang T, Feng W, Li C, Li F. Sub-10 nm hexagonal lanthanide-doped NaLuF4 upconversion nanocyrstals for sensitive bioimaging in vivo. Journal of the American Chemical Society. 2011.
6. Wang F, Banerjee D, Liu Y, Chen X, Liu X. Upconversion nanoparticles in biological labeling, imaging, and therapy. Analyst. 2010; 135:1839-1854.
7. Lim SF, Riehn R, Ryu WS, Khanarian N, Tung C, Tank D, Austin RH. In vivo and scanning electron microscopy imaging of upconverting nanophosphors in Caenorhabditis elegans. Nano Letters. 2006; 6: 169-174.
8. Wang C, Tao H, Cheng L, Liu Z. Near-infrared light induced in vivo photodynamic therapy of cancer based on upconversion nanoparticles. Biomaterials. 2011.
9. He X, Gao J, Gambhir SS, Cheng Z. Near-infrared fluorescent nanoprobes for cancer molecular imaging: status and challenges. Trends in Molecular Medicine. 2010; 16: 574-583.
10. Friedrich M, Nozadze R, Gan Q, Zelman-Femiak M, Ermolayev V, Wagner TU, Harms GS. Detection of single quantum dots in model organisms with sheet illumination microscopy. Biochemical and biophysical research communications. 2009; 390: 722-727.
11. Weigt S, Huebler N, Strecker R, Braunbeck T, Broschard TH. Zebrafish (Danio rerio) embryos as a model for testing proteratogens. Toxicology. 2011.
12. Ingham PW. The power of the zebrafish for disease analysis. Human molecular genetics. 2009; 18: R107.
13. Eimon PM, Ashkenazi A. The zebrafish as a model organism for the study of apoptosis. Apoptosis. 2010; 15: 331-349.
14. Parng C, Seng WL, Semino C, McGrath P. Zebrafish: a preclinical model for drug screening. Assay and drug development technologies. 2002; 1: 41-48.
15. McGrath P, Li CQ. Zebrafish: a predictive model for assessing drug-induced toxicity. Drug discovery today. 2008; 13: 394-401.
16. Kari G, Rodeck U, Dicker A. Zebrafish: an emerging model system for human disease and drug discovery. Clinical Pharmacology & Therapeutics. 2007; 82: 70-80.
17. Fako VE, Furgeson DY. Zebrafish as a correlative and predictive model for assessing biomaterial nanotoxicity. Advanced drug delivery reviews. 2009; 61: 478-486.
18. Fent K, Weisbrod CJ, Wirth-Heller A, Pieles U. Assessment of uptake and toxicity of fluorescent silica nanoparticles in zebrafish (Danio rerio) early life stages. Aquatic Toxicology. 2010; 100: 218-228.

19. Cheng J, Chan CM, Veca LM, Poon WL, Chan PK, Qu L, Sun YP, Cheng SH. Acute and long-term effects after single loading of functionalized multi-walled carbon nanotubes into zebrafish (Danio rerio). Toxicology and applied pharmacology. 2009; 235: 216-225.

20. Usenko CY, Harper SL, Tanguay RL. In vivo evaluation of carbon fullerene toxicity using embryonic zebrafish. Carbon. 2007; 45: 1891-1898.

21. Cheng J, Flahaut E, Cheng SH. Effect of carbon nanotubes on developing zebrafish (Danio rerio) embryos. Environmental Toxicology and Chemistry. 2007; 26: 708-716.

22. Bai W, Zhang Z, Tian W, He X, Ma Y, Zhao Y, Chai Z. Toxicity of zinc oxide nanoparticles to zebrafish embryo: a physicochemical study of toxicity mechanism. Journal of Nanoparticle Research. 2010; 12: 1645-1654.

23. Huang H, Huang C, Wang L, Ye X, Bai C, Simonich MT, Tanguay RL, Dong Q. Toxicity, uptake kinetics and behavior assessment in zebrafish embryos following exposure to perfluorooctanesulphonicacid (PFOS). Aquatic Toxicology. 2010; 98: 139-147.

24. Petit N, Lescure A, Rederstorff M, Krol A, Moghadaszadeh B, Wewer UM, Guicheney P, Selenoprotein N. An endoplasmic reticulum glycoprotein with an early developmental expression pattern. Human molecular genetics. 2003; 12: 1045.

25. Choi JE, Kim S, Ahn JH, Youn P, Kang JS, Park K, Yi J, Ryu DY. Induction of oxidative stress and apoptosis by silver nanoparticles in the liver of adult zebrafish. Aquatic Toxicology. 2010; 100: 151-159.

26. He M, Huang P, Zhang C, Hu H, Bao C, Gao G, He R, Cui D. Dual Phase-Controlled Synthesis of Uniform Lanthanide-Doped NaGdF4 Upconversion Nanocrystals Via an OA/Ionic Liquid Two-Phase System for In Vivo Dual-Modality Imaging. Advanced Functional Materials. 2011.

27. He M, Huang P, Zhang C, Chen F, Wang C, Ma J, He R, Cui D. A general strategy for the synthesis of upconversion rare earth fluoride nanocrystals via a novel OA/ionic liquid two-phase system. Chemical Communications. 2011.

28. Zhang C, Chen J. Facile EG/ionic liquid interfacial synthesis of uniform RE3+ doped NaYF4 nanocubes. Chem Commun. 2009; 46: 592-594.

29. Yang J, Sargent E, Kelley S, Ying JY. A general phase-transfer protocol for metal ions and its application in nanocrystal synthesis. Nature materials. 2009; 8: 683-689.

30. Deniziak M, Thisse C, Rederstorff M, Hindelang C, Thisse B, Lescure A. Loss of selenoprotein N function causes disruption of muscle architecture in the zebrafish embryo. Experimental cell research. 2007; 313: 156-167.

31. Yeo M, Kang M. Effects of nanometer sized silver materials on biological toxicity during zebrafish embryogenesis. Bulletin-Korean Chemical Society. 2008; 29: 1179.